

Application of silver-, iron-, and chitosan- nanoparticles in wastewater treatment

M.M. Naim^a, A.A. El-Shafei^{b,*}, M.M. Elewa^{c,*}, A.A. Moneer^d

^aFaculty of Engineering, Alexandria University, Alexandria, Egypt, Email: monanaim66@yahoo.com

^bFaculty of Agriculture, Alexandria University, Alexandria, Egypt, Email: ahmed.elshafi@alexu.edu.eg

^cArab Academy for Science, Technology and Maritime Transport, Alexandria, Egypt, Email: mahmoud.elewa@gmail.com

^dNational Institute of Oceanography and Fisheries, Alexandria, Egypt, Email: yrvah@yahoo.com

Received 30 July 2016; Accepted 5 November 2016

ABSTRACT

Silver nanoparticles (Ag-NPs) play an important role in the electronic industry, whereas, Zerovalent iron (ZVI) has been widely investigated for environmental remediation due to its fairly strong reducing power and its ability to adsorb an array of important contaminants such as heavy metals and metalloids, while, chitosan nanoparticles (CS-NPs) have proven efficacy in removal of heavy metals, dyes and phenols from wastewater. In the present work, chemical methods have been conducted to prepare nanoparticles made from silver, iron, and chitosan. Ag-NPs were prepared from AgNO₃ as starting material then the particles obtained were coated on filter paper; also, a cellulose acetate (CA) membrane was prepared after mixing the casting solution with Ag-NPs, then both subjected to *Escherichia (E.) coli* bacteria for testing their ability to destroy the bacteria. The *E. coli* was prepared according to a standard procedure and the colonies counted before and after treatment with treated filter paper and membrane. It is noteworthy that the present work contains a simple new method to prepare Ag-NPs. Results proved that Ag-NPs destroy the *E. coli* bacteria completely at room temperature in both filter paper and CA membrane. Also, Nano iron (nZVI) was prepared by reduction of ferric chloride by sodium borohydride, then filtered and used to remove Cu(II) ions from aqueous solution. CS-NPs were prepared by two methods, first by preparation of low molecular weight chitosan (LWCS) followed by its degradation to CS-NPs using different concentrations of H₂O₂ solution. The second method was done by preparing CS-NPs using AgNO₃. The CS-NPs membrane was able to biosorb 70.68 and 42.1% of NaCl from a 9.38 and 15.2 g/L salt solution respectively, whereas biosorption of CuSO₄ was 59.8% from 12.5 g/L solution, due to the presence of numerous functional groups besides the amino and hydroxyl groups.

Keywords: Nanoparticles; Wastewater treatment; *Escherichia coli*; Nanosilver; Cupric ions; Nano-zero valent iron; Nanochitosan

1. Introduction

Nanoparticles (NPs) are expected to play a crucial role in water purification [1]. The environmental fate and toxicity of a material are critical issues in materials selection and design for water sanitization. Most likely nanotechnology is superior to any different systems utilized as a part of water treatment [2]. The expulsion of bacteria from water is a crit-

ical procedure process for drinking and sanitation systems especially against concerns on growing outbreaks of water borne diseases [3,4]. Some conventional substance disinfectants (free chlorine, chloramines, and ozone) are now generally utilized as a part of the water business; alarmingly huge numbers of these are cancer-causing agents [5]. Furthermore, the resistance of microorganisms to these normal substance disinfectants is expanding; prevalent choices are in this way essential. The improvement of nano-science and

*Corresponding author.

Presented at the EDS conference on Desalination for the Environment: Clean Water and Energy, Rome, Italy, 22–26 May 2016.

nanotechnology inside the most recent decades furnishes chances to manage this issue. To this end, various NPs, for example, Ag, Cu, ZnO, and TiO₂, indicate high lethality to a wide range of pathogens and have been contemplated as antibacterial operators [6–8]. The iron NP innovation has gotten impressive consideration for its potential applications in groundwater treatment and site remediation. Late studies have exhibited the adequacy of nZVI for the change of halogenated natural contaminants and overwhelming metals [9]. CS-NPs show significant adsorption potential for the removal of various aquatic pollutants. They play an important role in removal of heavy metals, dyes and phenols from water [10–12].

Stable Ag-NPs suspension via the reduction of AgNO₃ using NaBH₄ and sodium citrate was prepared by Wang et al. [13]. Ag-NPs prepared by the AgNO₃ in PVP aqueous solution. The reaction was allowed to proceed, while being continually stirred, at a temperature of 25°C. The silver particle suspension was purified from ionic excess using a stirred membrane filtration cell with a regenerated cellulose membrane. The washing procedure was repeated until the conductivity of the supernatant solution stabilized. The authors concluded that the procedure adopted in this work enabled one to produce stable Ag particle suspensions.

A practical and convenient method to prepare stable colloidal Ag-NPs for use in printed electronic circuits was described by Natsuki and Abe [14]. The method uses a dispersant and two kinds of reducing agents including 2-(dimethylamino) ethanol, which play important roles in the reduction of Ag ions in an aqueous medium. This method presented significant advantages over previous ones including short reaction times, small and relatively uniform particles with a diameter less than 10 nm, and that the reaction proceeded rapidly at room temperature and organic solvents are not used. In addition, the resulting particles were easily separated from the reaction mixture. Kora et al. [15] prepared Ag-NPs through UV photo-reduction of a AgNO₃ aqueous solution, containing ethanol and SDS. All the solutions were prepared in ultra-pure water using an UV digester equipped with a high pressure mercury lamp of 500 W power, used as a source for UV light.

Yang et al. [16] synthesized nano iron/mesocarbon microbead composites from a coal tar pitch by heating at 415°C with ferrocene under pressure. The resulting composites were characterized by SEM, TEM, XRD, and EDS. It was found that the nanoiron particles were of sizes 10–40 nm and mainly existed in the form FeO and Fe_{1-x}S, and that the addition of ferrocene introduced a tendency to order in the micro-texture of spheres. Lee et al. [17] investigated the synthesis of nano size iron particles using a borohydride reduction of ferric ion in the presence of a solvent containing carboxyl groups. Stable and enhanced dispersion of iron NPs was achieved using a multi-component system of ferric ion, water and acetone. The latter retarded borohydride's reduction potential, resulting in more oxidized iron phase. The particles had an average size 60–80 nm. Song et al. [18] also synthesized nano-sized iron for reductive dechlorination of chlorinated solvents, using NaBH₄ in reducing Fe³⁺ in aqueous solution. They investigated a wide range of synthesis conditions including concentration of the reagents, reagent feeding rate, and solution pH, in an aque-

ous system under anaerobic condition. Wang and Zhang [19] synthesized Pd/Fe⁰ by NaBH₄ reduction of an iron salt (FeCl₃·6H₂O) in an aqueous phase, and used them as reductants for TCE and polychlorinated biphenyl mixture. Many reports appeared on the use of nano-sized iron to treat various types of contaminants included chlorinated ethylenes [20–22], chlorinated methanes [23,24], chlorinated benzenes [20,25], chromium [26,27], lead [26,27], and nitrate [28].

Mueller and Nowack [29] reported in a recent in depth report (observatory NANO focus report 2010) on nZVI the solution for water and soil remediation, in which they stated that major concerns were the limited mobility and life time of nZVI. They also gave an overview over the characteristics and application of nZVI and summarized the experiences on ground water remediation with nZVI in Europe. Sun et al. [9] conducted a systematic characterization of nZVI prepared by reduction of ferric iron with NaBH₄, in which particle size, size distribution and surface composition were characterized by TEM, XRD, HR – XPS, XANES and acoustic/electroacoustic spectrometry. An efficient way to immobilize nZVI in an alginate bead support material was developed by Kim et al. [30] in which both Fe₃ and Be₃ as the cross-linking cations were used. The effectiveness of the immobilized nZVI on the dechlorination of TCE was tested. They concluded that nZVI was efficiently immobilized in alginate bead and that the latter can be used efficiently in the dehalogenation of chlorinated solvents. Hwang et al. [31] studied the mechanism of nitrate reduction by nZVI which was prepared by chemical reduction without a stabilizing agent. The nZVI had great ability to reduce nitrate. However, the question of what end product results from nitrate reduction by nZVI has sparked controversy. FeCl₃, Cu(II) chloride and NaBH₄ were used for nZVI and Fe/Cu bimetal synthesis. Liu et al. [32] reported that nZVI was successfully immobilized on epichlorohydrine/CS beads for reduction of Cr(VI) from wastewater. The study demonstrated that the aforementioned beads could become an effective and promising technology for in situ remediation of Cr(VI).

The high adsorption potential of CS for heavy metals can be attributed to high hydrophilicity due to large number of hydroxyl groups of glucose units, presence of a large number of functional groups, high chemical reactivity of these groups, and flexible structure of the polymer chain [10]. Szeto et al. [33] invented a new method for preparing CS-NPs. The method uses the nano cavity technology so as to obtain pure CS-NPs and pure CS-NPs latex in a simple way. The method included dissolving CS in a dilute acid solution, then depositing it rapidly with an alkaline solution after which the deposit is washed with deionized water until neutrality followed by subjecting the deposit to ultrasonic cavity treatment, whereby it is crushed into NPs to give CS-NP latex. A CS nano dispersion with a narrow size distribution based on ionic gelation was studied for the removal of anionic dyes by Momenzadeh [34] and investigated the influence of various experimental conditions on the adsorption capacity of dissolved CS and of the CS nano dispersion. The CS-NPs showed much higher adsorption capacity and faster adsorption kinetics than dissolved CS. Yang et al. [35] used LWCS in the preparation of nano CS by dissolving CS followed by adding H₂O₂ and heating while stirring then vacuum fil-

tration. The nano CS was then applied to wool fabric to provide better antibacterial and shrink proof properties, then washing not less than 20 times. In a review by Zhao et al. [36] the preparation of CS nano structure and their application for encapsulating and immobilizing bioactive ingredients was summarized. They reviewed the preparation of CS-NPs by the ionic gelation method and the inverse micellar method as well as the preparation of CS nanofibres and the encapsulation of bioactive ingredients and their immobilization were also discussed. They concluded that micro/nano-structured CS can be used readily as bioactive ingredients carriers. However, most of the mentioned studies were still at the laboratory level. Yuwei and Jianlong [37] prepared magnetic CS-NPs and applied them in the removal of Cu(II) ions from aqueous solution. The experimental results showed that the particles were super-paramagnetic. The EDS images confirmed the presence of Cu(II) on the surface of magnetic CS-NPs. The maximum sorption capacity was calculated to be 35.5 mg/g using the Langmuir isotherm model. The particles were prepared by chemical co-precipitation of Fe₂ and Fe₃ ions by NaOH in the presence of CS, followed by hydro-thermal treatment. Huang et al. [38] studied the effect of LWCS anticreasing treatments of cotton fabric. The addition of LWCS increased the tensile strength retention and creasing resistance of the treated fabrics. They used H₂O₂ to degrade CS to LWCS.

The aim of the present work is to prepare NPs of Ag, Fe and CS by chemical methods to be used in wastewater treatment, to test removal of *E. coli* bacteria by Ag-NPs coated papers and Ag-NPs membrane, to study kinetic of removal Cu(II) by nZVI, and to investigate dialyzing aqueous NaCl and CuSO₄ solutions and in concomitantly functioning as affinity membranes for the adsorption of both NaCl and CuSO₄ from their solutions.

2. Materials and methods

2.1. Synthesis of nano silver particles

AgNO₃ (provided by S.C.O. chemicals, Egypt) was used as a source for Ag metal. Glucose was used for reduction of AgNO₃·NaOH (produced by SIC El Salam for chemical

industries, Egypt) was used to accelerate the reaction, as well as to act as dispersant for the particles to prevent their agglomeration. PVA (produced by LobaChemie (Mumbai, India (D.P = 1700–1800)) was used as an organic polymer to assist in preventing agglomeration.

The method of preparation of Ag-NPs consisted of several steps as follows: two solutions (1&2) were prepared separately and added to each other (Table 1). The first one is AgNO₃ solution and the other is a mixture of PVA, glucose, NaOH and distilled water, this mixture was stirred well while heating to 60–80°C for complete dissolution. AgNO₃ solution was then added drop by drop to the aforementioned mixture while stirring and heating to 60°C for 10 min. The whole mixture was then left to cool. Finally, the solid particles were washed with distilled water and centrifuged using a table-top centrifuge (model plc.03, serial no. 808561, Gemmy industrial corp., power: 220v /50Hz, 0.65A) to make sure that no traces of NO₃ ion were present.

2.1.1. Preparation of Ag-NPs coated paper

The washed particles suspension was filtered a number of times as shown in Table 1, then left to air-dry followed by coating the filter papers by Ag-NPs. The air-dried particles were subjected to SEM examination.

2.1.2. Preparation of Ag-NPs membrane

CA (packed and distributed by El-Gomhouria. Pharmaceutical Co. Code No. 109460, Batch No. 149756940) was used as a polymer. DMF (produced by El-Nasr pharmaceutical chemicals Co.) was used as solvent. The Ag-NPs prepared as shown in Table 1 (three routes) were used in preparing the membranes.

The first step was to fabricate the CA membrane by adding the components in a dry glass-stoppered bottle and stirring well, then covering the bottle, and the whole left for complete dissolution and removal of air bubbles to take place. The second step Ag-NPs was added to the mixture in the beaker then stirred and left to allow air bubbles to escape, after which the membrane was cast. The membranes were immersed in distilled water and the latter continually changing the water.

Table 1
Conditions of experiments for preparation of Ag NPs

Solution	Chemicals used	Composition		
		(Composition 1)	(Composition 2)	(Composition 3)
(1)	AgNO ₃ (g)	6.8	6.8	6.8
	Distilled water (ml)	40	40	40
(2)	PVA (g)	2	3	1
	Glucose (g)	2	3	2
	NaOH (g)	2	3	2
	Distilled water (ml)	120	120	120
	Time of centrifugation (h)	1.6	3	3.3
	Time of washing by centrifuge (h)	0.5	1	0.5
	Number of filtration used	5	3	5

2.1.3. Application of nano-silver

2.1.3.1. Combatting Escherichia coli bacteria

A shaking flask method was used to determine the antibacterial activity of the coated paper with Ag-NPs and the membrane. Gram-negative *E. coli* (ATCC6538) was used, and its samples with 104 CFU/cell were prepared using sterile distilled water. In the antibacterial activity test, 0.1 g paper sample and 0.1 g of membrane were added into the above solutions. They were then immersed in a water bath shaker at 37°C for 24h. For determining the actual number of microorganism colonies, 0.1 mL of each culture was transferred and seeded on an agar plate, and the plate was then kept in an incubator at 37°C for 24 h. The number of the colonies was counted, and the inhibition rate (IR) of the bacteria growth was calculated using the following equation:

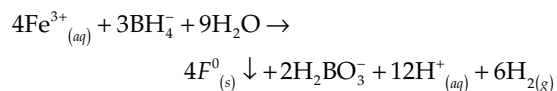
$$IR (\%) = \frac{N_0 - N}{N_0} \times 100$$

where N_0 and N are the number of the colonies detected from the blank and coated filter paper, and also for the membrane without and with Ag-NPs, respectively. Cell growth was monitored by measuring the optical density at 620 nm with a microtiter ELISA Reader (Molecular Devices Emax; Sunnyvale, CA, USA).

2.2. Synthesis of nano zero valent iron particles

NaBH_4 (provided by Oxford laboratory reagent, India). FeCl_3 (produced by SAS chemicals Co. Mumbai, India). Ethanol (95%) (Provided by Adwic, El-Nasr pharmaceutical chemical Co.).

nZVI particles prepared by reduction method using two main chemicals which were FeCl_3 and NaBH_4 followed the method proposed by Sun et al. [9]. The NaBH_4 functions as a reducing agent for the FeCl_3 in form of solution to produce nZVI by mixing equal volumes of 0.2 M NaBH_4 and 0.05 M FeCl_3 . nZVI particles were synthesized in the laboratory via the following reaction:



The borohydried solution was slowly added into the iron chloride to a flask reactor with three open necks as illustrated in Fig. 1. The central neck was fitted with a mechanical stirrer. Immediately after the first drop of reducing agent into iron solution, black particle appeared. Then further mixing for 60 min produce the maximum yield of black iron particles. Particles were then separated from the solution by vacuum filtration using What-mann cellulose nitrate membrane filter (0.2 mm). The solid particles were washed three times with absolute ethanol to remove all water. This washing process is probably the key step of synthesis since it prevents the rapid oxidation of nZVI. For storage, a thin layer of ethanol added to preserve the nano iron particles from oxidation.

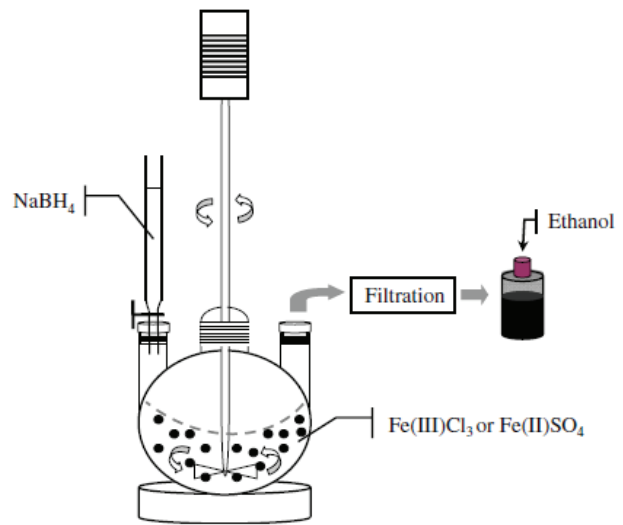


Fig. 1. Experimental setup for iron nanoparticle synthesis (adapted from Sun et al. [9]).

2.1.1. Application of nZVI particles

CuSO_4 (produced by Chemajet Chemicals Co., Egypt) was used as a source of copper ions. Batch experiments were carried out to evaluate the efficiency of nZVI particles for adsorb Cu(II) from CuSO_4 solution with different initial concentrations. Batch adsorption experiments were conducted using a known amount of the prepared adsorbent and metal ions solution at the working pH at various time intervals. Samples were collected after shaking in a rotary shaker at 200 rpm then filtered using 0.2 μm and the concentrations of the studied metal ions were determined. After subjected the nano-iron to solution of Cu we noticed that the concentration of Cu in reduced.

The metal ions concentration in the solution determined according to APHA [39] using atomic absorption spectrometer (Varian Spectra, AAS 220) equipped with deuterium arc background corrector. The amount of metal ions adsorbed per unit mass of the adsorbent evaluated by using the following mass balance equation,

$$q_e = \frac{(C_i - C_e) V}{W} \quad (1)$$

where q_e is the equilibrium adsorption capacity (mg/g), C_i and C_e are the initial and equilibrium liquid-phase concentrations of solute in aqueous solution (g/L), respectively. V is the liquid phase volume (L) and W is the mass of sorbent used (g).

Kinetic model, such as the pseudo-first-order kinetic and pseudo-second-order kinetic were applied to the experimental data to elucidate the adsorption mechanism. Batch tests performed to determine kinetics of adsorption. For this purpose, the optimum dose of the adsorbent added into 10 mL of metal solution at the effective pH value and initial metal concentration of 30 mg/L. At pre-decided intervals of time, the solutions were separated from the adsorbent and analyzed to determine the uptake of metal ions. Adsorption isotherm studies carried out with different initial con-

centrations of metal ions from 30 mg/L to 120 mg/L at the adsorption optimum pH and dose. All the investigations carried out in duplicate to confirm reproducibility of the experimental results.

2.3. Preparation of Nano-chitosan particles

Shrimp shells were obtained from the local fish market. NaOH (packed by B.D. Lab., Egypt) was used for preparation of CS from shrimp shells. H₂O₂ (produced by Luna Pac, Egypt, Vol. % 20 and 30) was used for degradation of the CS molecular chain. Ethanol (provided by Adwic, El-Nasr pharmaceutical chemicals Co., concentration 98%) was used to precipitate the low molecular weight CS (LWCS). Acetic acid (produced by Al-Alamia pharmaceutical chemicals Co., Egypt) was used for dissolving CS to obtain a CS solution. HCl (packed by B.D. Lab., Egypt with concentration 36%) was used as a catalyst for hydrolyzing CS.

Preparation of CS-NPs was completed in three successive steps; the first step was the preparation of CS followed by preparation of LWCS from which the nano-particles of CS was prepared by method 1 as shown in (Fig. 2a).

2.3.1. Preparation of Chitosan (CS)

The shrimp shells were washed after removing any adhering flesh, then left to air-dry. 20 g were then dissolved in 400 ml of 50% NaOH solution, and then heated until boiling with stirring, at constant volume for 2 h. The mixture was left to cool, then the solution was decanted and the solid washed until neutral, air dried and weighed (Fig. 2a).

2.3.1.1. Preparation of LWCS

2 g of CS were dissolved in 100 ml 0.1 M HCl and stirred for 30 min, then H₂O₂ was added in one of two volumes (20 or 30%), the mixture was heated at 60°C for 2 h. Ethanol was added to the solution to precipitate the LWCS, after which it was filtered on 2 filter papers, air-dried, then weighed (Fig. 2a).

2.3.2. Preparation of Nano-Chitosan

Method 1 1.625 g of LWCS were dissolved in 1000 ml of 2% acetic acid and stirred for 30 min until dissolution. 100 ml of solution were placed in an ice-water bath and placed in an ultra-sonicator (Lab Sonic LBS1-0.6, Power supply 100W), for 30 min., 2% NaOH solution was added to neutralize the acidity of the solution, then placed in an ice-water bath until a deposit was obtained (Fig. 2a).

Method 2 0.3 g of CS were dissolved in 100 ml of 0.3% acetic acid solution under mechanical agitation (300 rpm), then 5 ml of 5% aqueous AgNO₃ solution quickly poured into the above CS solution. Agitation was continued for 4 h until the solution became slightly red, and then 5% NaOH solution were quickly added until deposit was obtained. The CS precipitate obtained was filtered. The brown CS deposit was repeatedly washed with deionized water until the filtrate became neutral. The dried CS deposit was then transferred into a 100 ml conical flask and deionized water added up to a total volume of 100 ml. The whole was placed in an ice-water bath, then placed in an ultra-sonicator with

a power of 25 W. Ultrasonication was conducted for 30 min to obtain the CS-NPs (Fig. 2a).

2.3.3. CS-NPs membrane fabrication

40 ml of 10% aqueous acetic acid were added to the CS-NPs and warmed while stirring until dissolution to a viscous rather translucent solution took place. The solution was then poured in a petri-dish ($D = 12$ cm) and left to air dry away from dust for a few days to form a membrane. The membrane was then peeled gently and a sufficient amount of 40% NaOH solution was poured onto the membrane and left for 24 h in the covered dish in order to neutralize the remaining acetic acid. The membrane was then washed well with distilled water and kept in a covered container in distilled water to which 1 drop of chloroform was added as preservative (Fig. 2b).

2.3.4. Dialysis and adsorption of CS-NPs membrane

To investigate the performance of the fabricated CS-NPs membrane in dialysis and adsorption and study whether dialysis was going to dominate chelation of the metals chosen or vice versa. Accordingly, a simple diffusion plexiglass test cell was devised and constructed, which was composed of two identical compartments separated by two frames in which the membrane is inserted by placing between the frames together with flexible plastic gaskets then the latter fitted into a channel midway between the two compartments such that the latter are totally separated from each other (hermetically sealed). The dimensions of the diffusion cell are length = 10 cm, width = 5.8 cm and height = 7 cm.

Into one compartment a known quantity of either aqueous NaCl or CuSO₄ solution are added such that the solution is appreciably higher than the membrane's top level, while an equal volume of distilled water is added to the second compartment. Magnetic stirring is started in both compartments, and the concentration is determined at different time intervals by sampling 2 ml. The Cu ions concentration in the solution determined according to APHA [39] using atomic absorption spectrometer (Varian Spectra, AAS 220) equipped with deuterium arc background corrector. NaCl concentration was measured using conductivity meter at regular time intervals.

3. Results and discussions

3.1. Nano silver

3.1.1. Characterization of Ag-NPs particles

The surface morphology of Ag-NPs characterized by SEM (JEOL JSM-5600 LV). Fig. 3a illustrates nano-silver embedded in the CA membrane. It is clear that NPs are very well dispersed and that their sizes are in the thereabouts of 44.3 to 69.62 nm. However, about a dozen of particles appear in the micrograph which is larger than the majority of NPs, reaching about 100–150 nm. This observation stresses the fact that dispersion and immobilization of the NPs in a membrane is a very good route for preventing

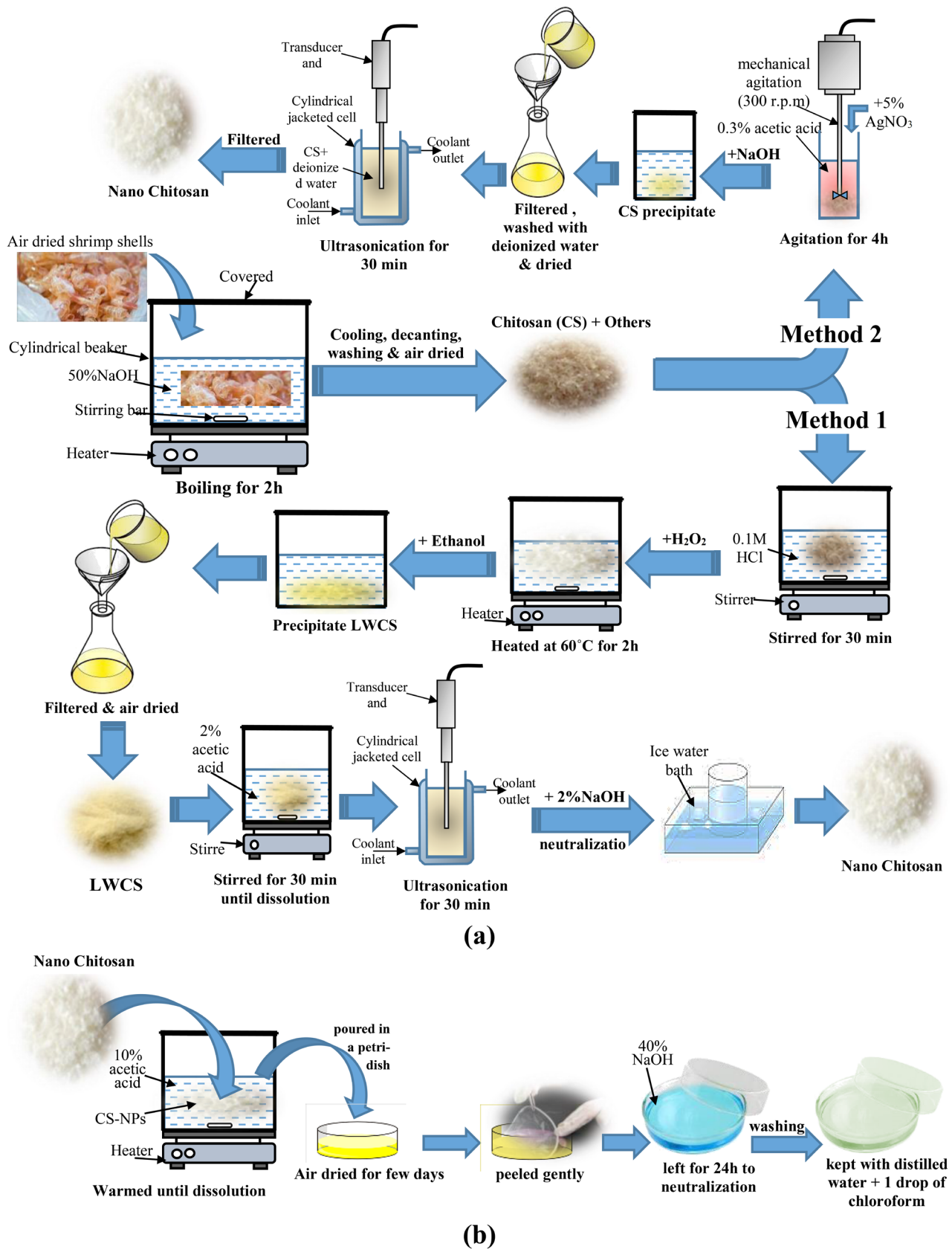


Fig. 2. Schematic diagram of preparation of Chitosan Nano – (a) particles, and (b) membrane.

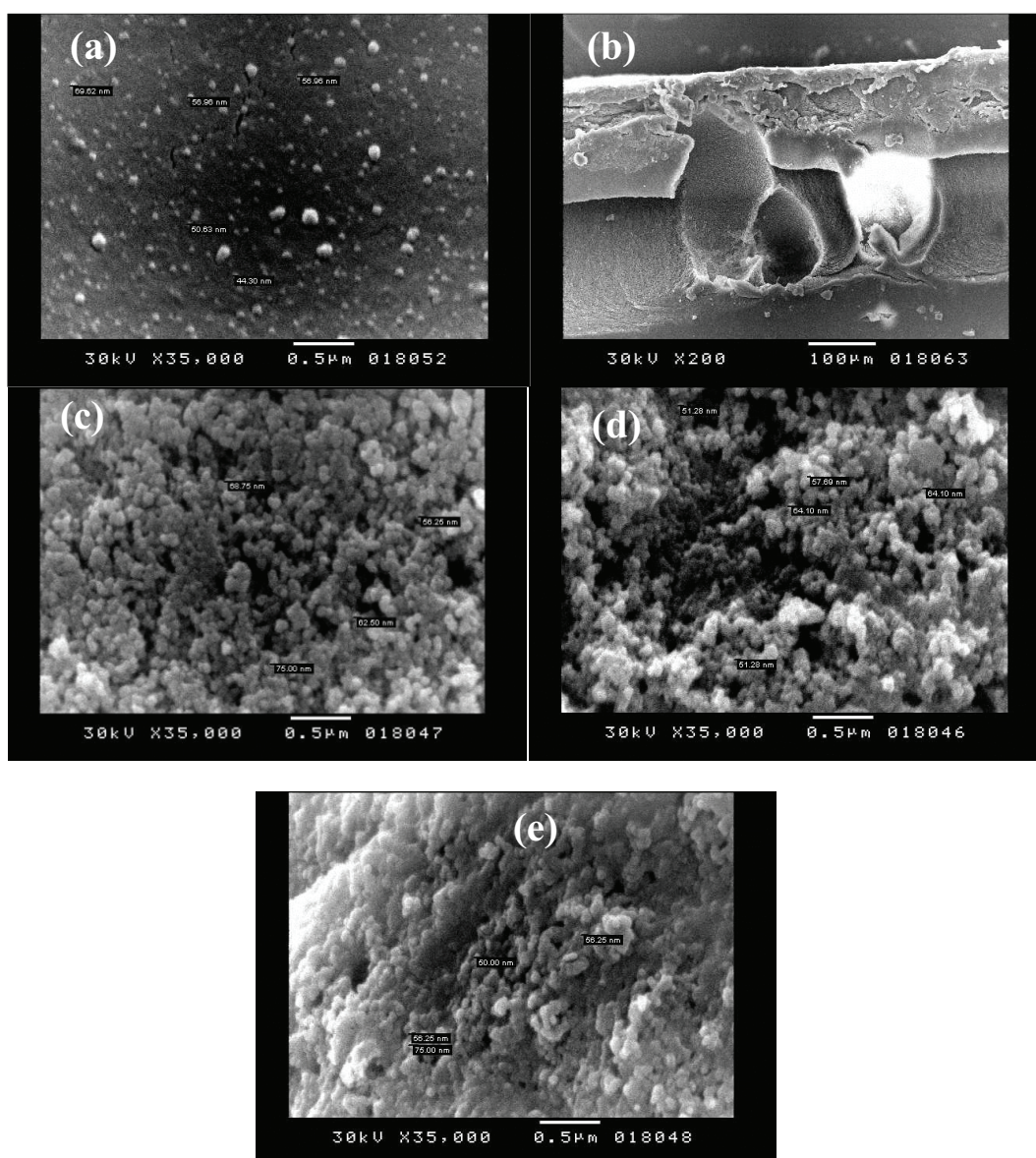


Fig. 3. SEM micrograph of Ag-NPs embedded in CA membrane: (a): top surface, (b): cross section of asymmetric CA membrane with shiny Ag-NPs on the top surface, and dispersed inside the membrane matrix, with a large cluster of shiny Ag-NPs embedded in a macro void, (c): Ag NPs prepared according to composition 2 (Table 1), (d): Ag-NPs prepared according to Composition 1 (Table 1), (e): Ag-NPs prepared according to composition 3 (Table 1).

agglomeration and loss of the NPs in case of utilizing the Ag-NPs in water treatment. Fig. 3b illustrates the cross sectional view of the membrane from which it is shown that NPs are distributed specially in the top skin layer. The membrane is seen to be formed of a thin top skin layer in which plenty of NPs are embedded followed by a transition layer that is partially filled with the NPs and partially filled with pores. The bottom layer following the transition layer is filled with macro-voids which contain evenly distributed NPs. However, a large cluster of shiny nano-Ag is embedded within the membrane matrix. To this end, it could be stated that the membrane could be used as an efficient UF membrane through which the permeating water becomes purified of fungi and bacteria such as *E. coli*.

Fig. 3c presents Ag-NPs prepared according to Composition 2 (Table 1) in which AgNO_3 is reduced by glucose in the presence of PVA and NaOH. It is obvious that the NPs are tremendous and that they are uniform to a great extent indicating that the method employed leads to the formation of Ag-NPs efficiently. It is worth noting that previous work was done using PVP and that PVA has never been used before. From Fig. 3c, it is clear that the NPs vary from 56.25 to 75.0 nm which are somewhat larger than the NPs embedded in the CA membrane presented in Fig. 3a, which points out the important of immobilizing the NPs in a membrane to avoid their agglomeration.

Fig. 3d presents the micrograph of Ag-NPs prepared according to composition 1, (Table 1) in which the quanti-

ties of PVA, glucose and NaOH are of lower quantity than composition 2 with respect to the quantity of AgNO_3 , but of identical ratios. An inspection of the figure indicates that the NPs are more or less agglomerated as compared to those in Fig. 3c. The NPs are more non-uniform when compared to Fig. 3c. This observation proves that composition 2 presents better quantities that lead to smaller and un-clustered NPs than composition 1. Accordingly, quantities of composition 2 are preferred and recommended. As to the particle size which is clarified in Fig. 3c, the particle sizes vary between 51.28 and 64.10 nm of particles present in the agglomerates.

Fig. 3e presents the micrograph of Ag-NPs prepared according to composition 3 (Table 1) using a lower quantity of PVA than in composition 1. Once more the particles are non-uniform and agglomerated (note: the left hand side of the figure). This observation points out the importance of the quantity of PVA polymer, which proves that on increasing its quantity from 1 to 2 to 3 g is an important reason leading to better distribution and immobilization of the NPs and less clustering of the particles; accordingly, a larger surface area of NPs per unit volume is offered on increasing the PVA, which makes the NPs more available for action. It is noticed that some particles in the clusters range between 50–75 nm.

3.1.2. Combatting *Escherichia coli* bacteria by Ag-NPs

The results proved that the coated filter papers with manufactured Ag-NPs by three composition as well as Ag-NPs membrane were destroyed the *E. coli* bacteria completely at room temperature with 100% IR.

3.2. Nano zero valent iron particles (nZVI)

3.2.1. Characterization of nZVI particles

The surface morphology of nZVI characterized by SEM (JEOL JSM-5600 LV). Fig. 4 presents the SEM images of the nZVI particle, which appeared as a spherical particle. It is clear that their size ranges between 37.97 and 44.30 nm and formed a chain-like aggregate attributed to the magnetic interactions between the adjacent metal particles this aggress with Zhang and Manthiram [40] and Taha and Ibrahim [41]. nZVI synthesized using this method tend to either agglomerate rapidly or react quickly with the surrounding media (e.g. dissolved oxygen or water), resulting in rapid decrease in mobility and reactivity He and Zhao [42].

3.2.2. Adsorption kinetic model

In order to formulate a pragmatic program for design, operation, and optimization, many kinetic models have been used to determine the intrinsic kinetic adsorption constants [43]. Traditionally, the adsorption kinetics of metal ions is described following the expressions originally given by Lagergren [43,44] which are special cases for the general Langmuir rate equation [45]. In order to distinguish a kinetic equation based on the adsorption capacity of a solid from one based on the concentration of a solution, Lagergren's first-order rate equation has been called pseudo-first-order [44] and Ho's second-order rate expression has been called

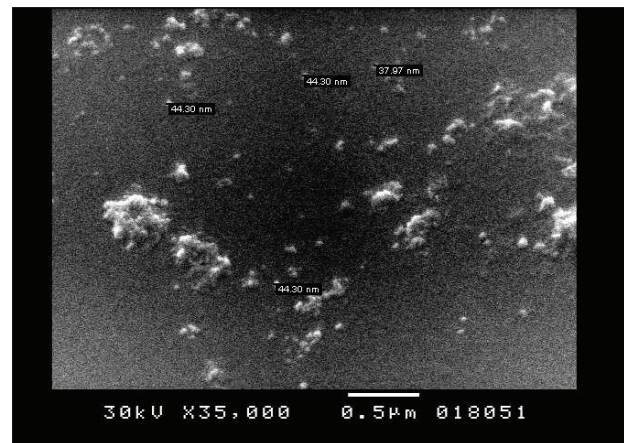


Fig. 4. SEM micrograph of nZVI showing some clusters of NPs.

pseudo-second-order [46]. The latter expression of Ho [46] has been widely applied to the sorption of metal ions and other species.

Accordingly, a simple kinetic analysis of adsorption is the pseudo-first-order equation in the form:

$$\frac{dq_t}{dt} = k_1(q_e - q_t) \quad (2)$$

where k_1 is the rate constant of pseudo-first-order adsorption, and q_e denotes the amount of adsorption at equilibrium.

After definite integration and applying the initial conditions: $q_t = 0$ at $t = 0$ and $q_t = q_t$ at $t = t$, Eq. (2) becomes:

$$\ln(q_e - q_t) = \ln q_e - k_1 t \quad (3)$$

In addition, a pseudo-second-order equation based on adsorption equilibrium capacity may be expressed in the form:

$$\frac{dq_t}{dt} = k_2(q_e - q_t)^2 \quad (4)$$

where k_2 is the rate constant of pseudo-second-order adsorption.

Integrating Eq. (4) and applying the initial conditions, Eq. (4) becomes:

$$\frac{1}{(q_e - q_t)} = \frac{1}{q_e} + k_2 t \quad (5)$$

or equivalently

$$\frac{t}{q_t} = \frac{1}{k_2 q_e^2} + \frac{1}{q_e} t \quad (6)$$

It should be noted that compared to Eq. (5), Eq. (6) has the advantage that k_2 and q_e can be obtained from the intercept and slope of plot t/q_t versus t and there is no need to know the q_e parameter (at equilibrium) beforehand [47,48]. However, in the present case q_e can be directly determined from the concentration-time plots. The fitting validity of these models is traditionally checked by linear plots of \ln

$(q_e - q_t)$ versus t and t/q_t versus t respectively [48]. From the slope and intersection of the straight line obtained, the corresponding constant values of the first- and second- order kinetic models at the temperatures studied, provides the respective kinetic constants k_1 and k_2 and the q_e parameters.

The experimental results show that the sorption of Cu^{2+} ions onto nZVI was rapid for the first 10 min and equilibrium was reached within 60 min. From Table 2, it is found that correlation coefficients values of pseudo-first order are low and the q_e values acquired by this method are contrasted with the experimental values. So the adsorption cannot be classified as first order.

Linear plot of t/qt vs. t is achieved according to Eq. (6) and the k and q_e values calculated from the slope and intercept of the plot. The pseudo second-order model considers the rate-limiting step in adsorption of $\text{Cu}(\text{II})$ is chemisorption and chemisorptive bonds involving sharing or exchange of electrons between adsorbate and the adsorbent, were applied. The results in Table 2 shows the experimental and calculated values of q_e agree with each other. The correlation coefficients for the second-order kinetic model were all greater than 0.98 indicating that the adsorption of $\text{Cu}(\text{II})$ obeyed the second-order kinetic model and the rate limiting step in adsorption of metals ions are chemisorption.

3.3. Applications of CS-NPs

3.3.1. Characterization of CS-NPs

Fig. 5a illustrates CS-NPs which are of size 37.88–60.61 nm. It is clear that the NPs are present as individual particles which are very well dispersed in the matrix and that no agglomeration whatever took place. However, it is noteworthy that the magnification in this micrograph is 50,000, which clarifies the presence of individual NPs of the CS-NPs.

Fig. 5b illustrates the micrographs of CS-NPs magnified 75,000 times. It is clear that The NPs are very fine, uniform and much smaller than these prepared by the previous method (17.07–21.95 nm), which should be very effective in wastewater treatment. Moreover, the NPs are very well dispersed and do not agglomerates. Fig. 5c presents CS-NPs at the same magnification (75,000) in which all the observations apply except that the particles are slightly smaller probably due to the lower concentration of H_2O_2 used in its preparation.

3.3.2. Dialysis and adsorption of CS-NPs Membrane

Concentration-time curves were plotted for the different experiments. Fig. 6 indicates that the concentration dropped

Table 2
Kinetic parameters for Cu^{2+} adsorption by nZVI particles

Pseudo-first order		Pseudo-second order	
q_e (mg/g) (calculated)	29.39	q_e (mg/g) (calculated)	21.5
k_1 (min^{-1})	0.1077	k_2 ($\text{g mg}^{-1}\text{min}^{-1}$)	0.0007
R^2	0.8143	R^2	0.9885

from 9.38 g NaCl/L solution to 2.9 g/L in 55 min, concomitantly, the distilled water compartment's salinity increased from zero to 2.9 g/L in the same time. This result shows that while one third the NaCl was dialyzed the remaining two thirds were adsorbed into the membrane pores and onto its surface. This result shows that the membrane functions as an adsorptive membrane, at the same time allows diffusion of some NaCl by dialysis. Accordingly, on the salt water side NaCl was reduced to less than one third its initial

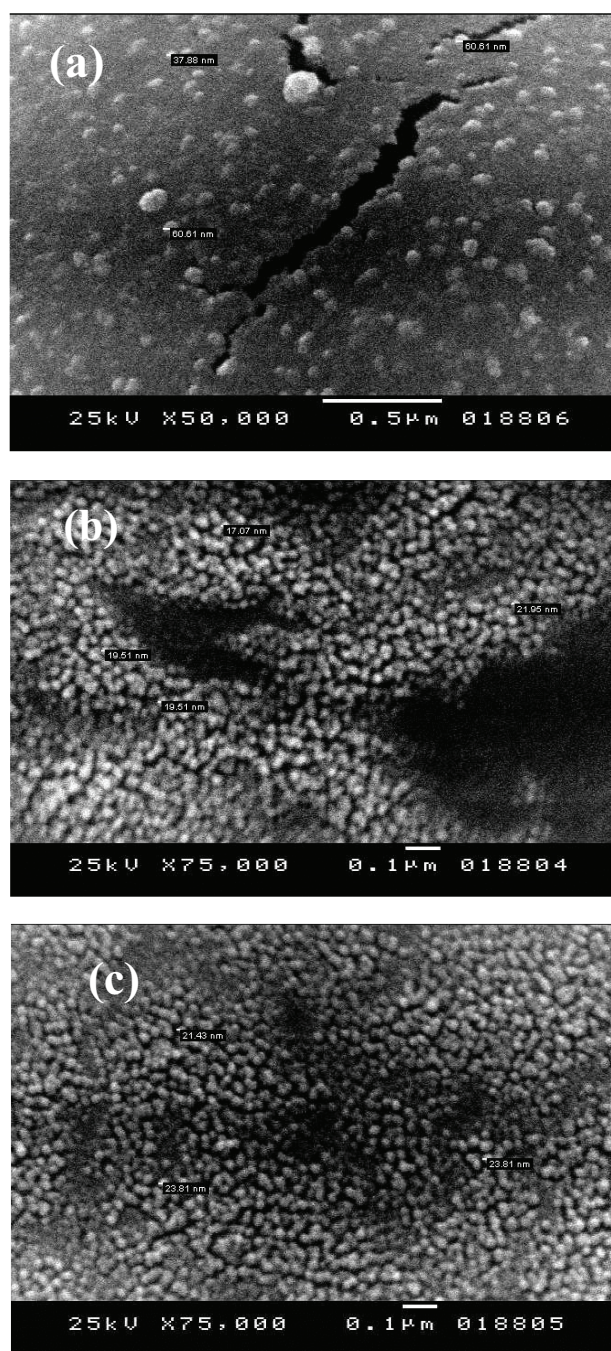


Fig. 5. SEM micrograph of CS-NPs: (a): obtained from method (2), (b): obtained from method (1), (c): obtained from method (1) with lower concentration of H_2O_2 .

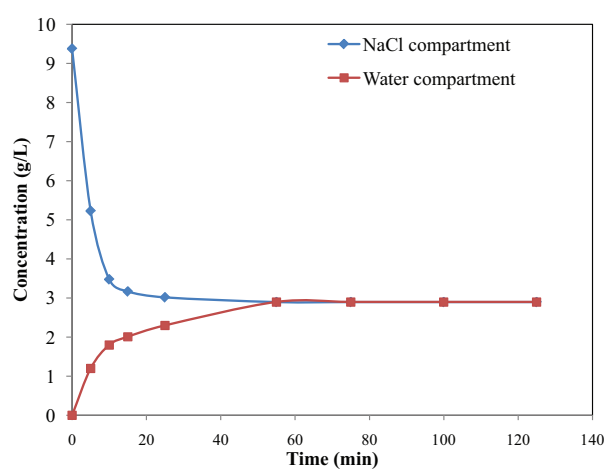


Fig. 6. Concentration-Time curves for the dialysis for NaCl through unused CS-NPs membrane prepared by method 1, $T = 30^{\circ}\text{C}$, NaCl concentration = 9.38 g/L.

concentration, which means that CS-NPs membrane, could contribute in desalination of brackish water. This result also suggests that subjecting the desalinated water to another stage can result in producing potable water, or that had the membrane area been larger, an even better result could have been achieved.

Fig. 7a shows the effect of increasing the initial concentration (C_i) of NaCl to 15.2 g/L. The concentration dropped to 8.8 g/L in 65 min, which is equivalent to a percent extraction through adsorption = 42.1%. This result compared to that of Fig. 6 proves that as C_i is increased, percent extraction is decreased, which is logic due to constancy of available functional groups due to the membrane area being equal in the two cases.

Fig. 7b presents the results of exchanging the initial contents of the two compartments. The result shows that a lower percent extraction was obtained (23%), due to the remaining vacant sites on the other side of the membrane becoming saturated.

Fig. 8a shows the result of diffusion experiment carried out with $\text{CuSO}_4 \cdot 5\text{H}_2\text{O}$ as solute. The figure proves that C_i dropped from 12.5 g/L to 5.025 g/L in 75 min at the same time no CuSO_4 dialyzed through the membrane, revealed by the zero concentration of the distilled water at all times. This result proves that the CuSO_4 was only adsorbed onto the CS-NPs membrane, which was also confirmed by the membrane becoming deep blue by time, leaving the solution a much paler blue than its initial color. Another conclusion is that no dialysis took place due to pore blocking on biosorption. The percent extracted CuSO_4 was about 60%. Again had the membrane area been larger, complete removal of CuSO_4 solution could have been achieved.

Fig. 8b shows what happened when the compartment contents were reversed keeping the membrane in place as it is. A new solution (12.5 g/L) and fresh distilled water were used and another experiment was conducted. It was realized that C_i dropped from 12.5 g/L to 10.05 g/L only and that the membrane color became a deeper blue. This result points out that the side on which adsorption took place was subjected initially in the previous experiment to surface

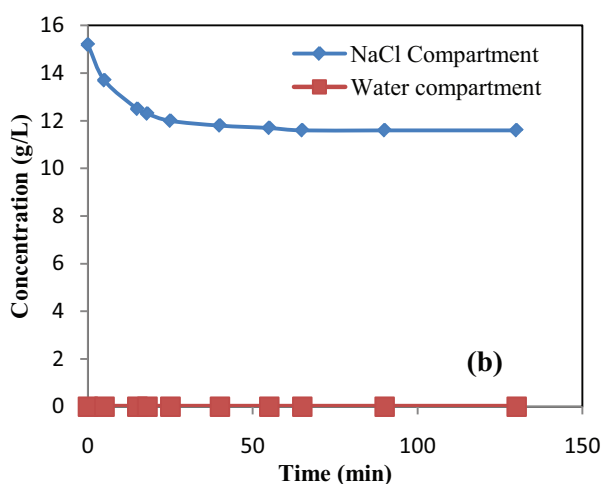
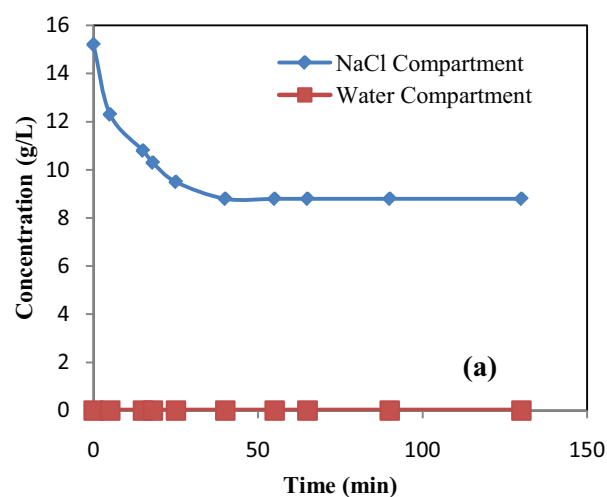


Fig. 7. Concentration-Time curves for the dialysis for NaCl through CS-NPs membrane, $T = 30^{\circ}\text{C}$, NaCl concentration = 15.2 g/L, (a): unused membrane prepared by method 2, (b): used membrane prepared by method 2.

adsorption and pore adsorption plus some adsorption on the farther side (as denoted by its blue color also), but that the farther side was still not saturated and that adsorption sites were still available in the second experiment though few, and percent extraction in this case was only about 20%. This result is very important in that it suggests that a continuous process may be designed with a multiple array of parallel membranes, between which the solution is allowed to flow along the membranes between each pair, so that the membranes become rapidly saturated by the solute. Later on, recovery of the solute may be accomplished by pumping dilute H_2SO_4 through the channels to dissolve the CuSO_4 once again for reuse as desired, and then the process is repeated.

It is noteworthy that the solutes are bound to the membrane surface and inside its pores by physico-chemical attraction between the abundant functional groups in the CS in particular and other contents such as proteins, lipids and pigments and inorganics which are mostly removed during its preparation from native chitin. It is also deduced that heavy metal ions are biosorbed to a greater extent than

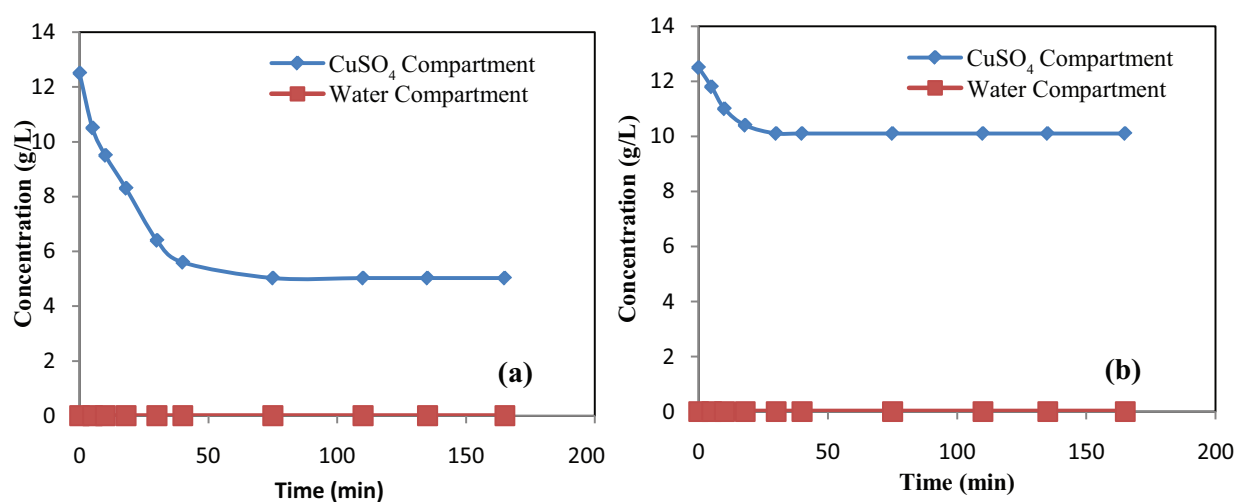


Fig. 8. Concentration-Time curves for the dialysis for CuSO_4 through CS-NPs membrane, $T = 30^\circ\text{C}$, NaCl concentration = 12.5 g/L , (a) unused membrane prepared by method 2, (b) used membrane prepared by method 2.

alkali metal ions, which is expected since CS is known for its great ability in chelating heavy metals from aqueous solution. The results prove that due to preferential biosorption, dialysis is either negligible or nil.

3.4. Kinetics of adsorption

The calculated results of the first-order rate equation showed that correlation coefficients values are low and the q_e values acquired by this method is contrasted with the experimental values. So the adsorption cannot be classified as first order. On the other hand the best linear fittings were detected using the pseudo-second-order kinetic model. It is known that the lone pair of electrons present in the amine ($-\text{NH}_2$) groups and lone pairs of electrons of the hydroxyl ($-\text{OH}$) groups can establish coordinate bonds with transition metal ions. It has been mentioned that first-order kinetic processes have been used for reversible reactions with an equilibrium being established between liquid and solid phases, whereas, the second-order kinetic model assumes that the rate-limiting step may be chemical adsorption [49]. It was found that the squares of the correlation factor (R^2) are all in the vicinity of 0.999, which proves that the pseudo-second-order kinetic model fits excellently to the obtained results, which suggests that the rate-limiting step may be the chemical adsorption (chemisorption) but not the mass transport. Table 3 presents k_2 and both experimental and calculated q_e for the different salts in the interaction of the salts to unused CS-NPs membrane using the Lagergren pseudo-second-order kinetic model. From the table it is observed that q_e experimental has a value not far from q_e calculated. The table also shows the computed values of k_2 which is the rate constant of the pseudo-second-order equation. Their values proved that k_2 is best when using CuSO_4 as solute since only 8.47 mm^2 of membrane area biosorb 1 mg of CuSO_4/min , on the other hand when using NaCl k_2 came out to be 60 and 23.7 at the lower and higher concentrations respectively, which means that a much larger membrane area is required to biosorb 1 mg of CuSO_4/min . However, at high NaCl concentrations, k_2 is much better

Table 3
 k_2 and q_e of the interaction of Cu (II)- and NaCl with CS membranes using the Lagergren pseudo-second-order model at 30°C

Membrane	Salt	q_e experimental mg/cm^2	q_e calculated mg/cm^2	K_2 $\text{mm}^2/\text{mg min}$
Unused CS-NPs	9.38 gNaCl/L	46.04	42.6	60
Unused CS-NPs	15.2 gNaCl/L	44.44	50.47	23.7
Used CS-NPs	15.2 gNaCl/L	24.3	28.13	40.1
Unused CS-NPs	12.5 g CuSO_4/L	51.9	64.93	8.47
Used CS-NPs	12.5 g CuSO_4/L	17.01	21.32	33.2

than at low concentration. This point proves that to unused CS-NPs membranes adsorb at higher concentrations both efficiently and rapidly. On reversing the adsorbate solutions and the distilled water in the compartments as explained previously, it is observed that for both NaCl and CuSO_4 , the k_2 values increased greatly from 23.7 to 40.1 $\text{mm}^2/\text{mg min}$ and from 8.47 to 33.21 $\text{mm}^2/\text{mg min}$ in case of NaCl and CuSO_4 respectively, which was expected due to the functional groups being less available.

4. Conclusions

From the present work, the following conclusions were arrived at:

1. AgNO_3 was reduced by glucose, and Ag-NPs were generated in the solution containing PVA. The produced Ag-NPs were used to destroy *E. coli* bacteria from water. The results proved that the coated filter papers with manufactured Ag-NPs by three compo-

sition as well as Ag-NPs membrane were destroyed the *E. coli* bacteria completely at room temperature with 100% IR.

- Nano scale zero valent iron (nZVI) particles prepared by reduction method using two main chemicals which were FeCl_3 and NaBH_4 , the produced nZVI was used to remove cupric ions taken as an example from heavy metals, efficiently from water in two stages and was still active.
- CS was prepared by de-acetylation of chitin in shrimp shells, and was degraded into LWCS using different concentrations of H_2O_2 solution (20% and 30%).
- CS-NPs were produced from LWCS by ultra sonication easily.
- It was concluded that copper (heavy metal) sulfate was adsorbed more rapidly than sodium (alkali metal) chloride, and that the CS NPs membrane, due to the presence of numerous functional groups besides the amino and hydroxyl groups, was able to biosorb 70.68% of NaCl from a 9.38 g/L salt solution, and 42.1% from a 15.2 g/L salt solution, whereas biosorption of CuSO_4 was 59.8% from a 12.5 g/L solution, while on reversal of the liquids in the compartments another 19.6% was extracted. It was also shown that the adsorption process was best described by the pseudo-second-order kinetic equation for both salts investigated, which proved that the rate-limiting step was chemisorption and not mass transport. A final conclusion is that biosorption takes place on the membrane surface and most importantly inside the pores of the membrane matrix, as proven by SEM micrographs.

Symbols

A	—	Ampere
Ag	—	Silver
AgNO_3	—	Silver nitrate
Ag-NPs	—	Silver nanoparticles
APHA	—	American Public Health Association
CA	—	Cellulose acetate
Cr	—	Chromium
CS	—	Chitosan
CS-NPs	—	chitosan nanoparticles
Cu	—	Copper
CuSO_4	—	Copper sulphate
DMF	—	Di-methyl formamide
<i>E. coli</i>	—	<i>Escherichia coli</i>
ELISA	—	Enzyme-linked immunosorbent assay
EDS	—	Energy Dispersive Spectrometer
FeCl_3	—	Ferric chloride
$\text{FeCl}_3 \cdot 6\text{H}_2\text{O}$	—	iron salt in an aqueous phase
HCl	—	Hydrochloric acid
H_2O_2	—	Hydrogen peroxide
H_2SO_4	—	Sulphuric acid
IR	—	Inhibition rate
LWCS	—	Low Molecular weight chitosan
ml	—	Milliliter
NaOH	—	Sodium hydroxide

NaBH_4	—	Sodium borohydride
NaCl	—	Sodium chloride
nm	—	Nano meter
NPs	—	Nanoparticles
nZVI	—	Nano-scale zero-valent iron
q_e	—	Equilibrium adsorption capacity (mg/g)
PVA	—	Poly vinyl alcohol
PS	—	Particle size
TiO_2	—	Titanium Dioxide
XANES	—	X-Ray absorption near edge structure
TCE	—	Trichloroethylene
SDS	—	sodium dodecyl sulfate
SEM	—	scanning electron microscopy
TEM	—	Transmission Electron Microscope
UV	—	Ultra violet
Pd/Fe ⁰	—	nanosized iron
XRD	—	X Ray Diffraction
HR – XPS	—	High Resolution X-Ray Photoelectron Spectroscopy
W	—	Watt
ZnO	—	Zinc Oxide
ZVI	—	Zero-valent iron
V	—	Volt
PVP	—	Poly vinyl pyrrolidone

References

- P.K. Stoimenov, R.L. Klinger, G.L. Marchin, K.J. Klabunde, Metal oxide nanoparticles as bactericidal agents, *Langmuir*, 18 (2002) 6679–6686.
- V.L. Colvin, The potential environmental impact of engineered nanomaterials, *Nat. Biotech.*, 21 (2003) 1166–1170.
- Q. Li, S. Mahendra, D.Y. Lyon, L. Brunet, M.V. Liga, D. Li, P.J.J. Alvarez, Antimicrobial nanomaterials for water disinfection and microbial control: Potential applications and implications, *Water Res.*, 42 (2008) 4591–4602.
- D. Gangadharan, K. Harshvardan, G. Gnanasekar, D. Dixit, K.M. Papat, P.S. Anand, Polymeric microspheres containing silver nanoparticles as a bactericidal agent for water disinfection, *Water Res.*, 44 (2010) 5481–5487.
- W. Kratschmer, L.D. Lamb, K. Fostiropoulos, D.R. Huffman, Solid C_{60} : a new form of carbon, *Nature*, 347 (1990) 354–358.
- H. Zhang, G. Chen, Potent antibacterial activities of Ag/ TiO_2 nanocomposite powders synthesized by a one-pot sol-gel method, *Environ. Sci. Technol.*, 43 (2009) 2905–2910.
- R. Dastjerdi, M. Montazer, A review on the application of inorganic nano-structured materials in the modification of textiles: Focus on anti-microbial properties, *Colloid Surface B.*, 79 (2010) 5–18.
- J.P. Ruparelia, A.K. Chatterjee, S.P. Duttagupta, S. Mukherji, Strain specificity in antimicrobial activity of silver and copper nanoparticles, *Acta Biomater.*, 4 (2008) 707–716.
- Y.-P. Sun, X.-q. Li, J. Cao, W.-x. Zhang, H.P. Wang, Characterization of zero-valent iron nanoparticles, *Adv. Colloid. Interfac.*, 120 (2006) 47–56.
- A. Bhatnagar, M. Sillanpää, Applications of chitin- and chitosan-derivatives for the detoxification of water and wastewater — A short review, *Adv. Colloid Interfac.*, 152 (2009) 26–38.
- M.N.V. Ravi Kumar, A review of chitin and chitosan applications, *React. Funct. Polym.*, 46 (2000) 1–27.
- G. Crini, P.-M. Badot, Application of chitosan, a natural aminopolysaccharide, for dye removal from aqueous solutions by adsorption processes using batch studies: A review of recent literature, *Prog. Polym. Sci.*, 33 (2008) 399–447.
- H. Wang, X. Qiao, J. Chen, S. Ding, Preparation of silver nanoparticles by chemical reduction method, *Colloid Surface A.*, 256 (2005) 111–115.

- [14] J. Natsuki, T. Abe, Synthesis of pure colloidal silver nanoparticles with high electroconductivity for printed electronic circuits: The effect of amines on their formation in aqueous media, *J. Colloid Interf. Sci.*, 359 (2011) 19–23.
- [15] A.J. Kora, R. Manjusha, J. Arunachalam, Superior bactericidal activity of SDS capped silver nanoparticles: Synthesis and characterization, *Mater. Sci. Eng. C.*, 29 (2009) 2104–2109.
- [16] Y. Yang, C. Wang, M. Chen, Preparation and structure analysis of nano-iron/mesocarbon microbead composites made from a coal tar pitch with addition of ferrocene, *J. Phys. Chem. Solids*, 70 (2009) 1344–1347.
- [17] J.-m. Lee, J.-h. Kim, J.-w. Lee, J.-h. Kim, H.-s. Lee, Y.-s. Chang, T.J. Nurmi, P.G. Tratnyek, Synthesis of Fe-nano particles obtained by borohydride reduction with solvent, Proc. Sixth International Conference on Remediation of Chlorinated and Recalcitrant Compounds B.M. Sass, ed., Battelle, Columbus, OH, Monterey, CA, 2008, Paper A-068.
- [18] H. Song, E.R. Carraway, Y.-H. Kim, Synthesis of nano-size iron for reductive dechlorination. 2. Effects of synthesis conditions on iron reactivities, *Environ. Eng. Res.*, 10 (2005) 174–180.
- [19] C.B. Wang, W.X. Zhang, Synthesizing nanoscale iron particles for rapid and complete dechlorination of TCE and PCBs, *Environ. Sci. Technol.*, 31 (1997) 2154–2156.
- [20] W. Zhang, C.B. Wang, H.L. Lien, Treatment of chlorinated organic contaminants with nanoscale bimetallic particles, *Catal. Today*, 40 (1998) 387–395.
- [21] H.L. Lien, W. Zhang, Nanoscale iron particles for complete reduction of chlorinated ethenes, *Colloid Surface A.*, 191 (2001) 97–105.
- [22] B. Schrick, J.L. Blough, A.D. Jones, T.E. Mallouk, Hydrodechlorination of trichloroethylene to hydrocarbons using bimetallic nickel-iron nanoparticles, *Chem. Mater.*, 14 (2002) 5140–5147.
- [23] H.L. Lien, W. Zhang, Transformation of chlorinated methanes by nanoscale iron particles, *J. Environ. Eng.*, 125 (1999) 1042–1047.
- [24] S. Choe, S.H. Lee, Y.Y. Chang, K.Y. Hwang, J. Khim, Rapid reductive destruction of hazardous organic compounds by nanoscale Fe⁰, *Chemosphere*, 42 (2001) 367–372.
- [25] Y. Xu, W. Zhang, Subcolloidal Fe/Ag particles for reductive dehalogenation of chlorinated benzenes, *Ind. Eng. Chem. Res.*, 39 (2000) 2238–2244.
- [26] S.M. Ponder, J.G. Darab, T.E. Mallouk, Remediation of Cr (VI) and Pb (II) aqueous solutions using supported, nanoscale zero-valent iron, *Environ. Sci. Technol.*, 34 (2000) 2564–2569.
- [27] S.M. Ponder, J.G. Darab, J. Bucher, D. Caulder, I. Craig, L. Davis, N. Edelstein, W. Lukens, H. Nitsche, L. Rao, Surface chemistry and electrochemistry of supported zerovalent iron nanoparticles in the remediation of aqueous metal contaminants, *Chem. Mater.*, 13 (2001) 479–486.
- [28] S. Choe, Y.Y. Chang, K.Y. Hwang, J. Khim, Kinetics of reductive denitrification by nanoscale zero-valent iron, *Chemosphere*, 41 (2000) 1307–1311.
- [29] N.C. Müller, B. Nowack, Nano zero valent iron—THE solution for water and soil remediation? in: Report of the Observatory NANO, 2010 1–34.
- [30] H. Kim, H.-J. Hong, J. Jung, S.-H. Kim, J.-W. Yang, Degradation of trichloroethylene (TCE) by nanoscale zero-valent iron (nZVI) immobilized in alginate bead, *J. Hazard. Mater.*, 176 (2010) 1038–1043.
- [31] Y.-H. Hwang, D.-G. Kim, H.-S. Shin, Mechanism study of nitrate reduction by nano zero valent iron, *J. Hazard. Mater.*, 185 (2011) 1513–1521.
- [32] T. Liu, Z.-L. Wang, L. Zhao, X. Yang, Enhanced chitosan/Fe⁰-nanoparticles beads for hexavalent chromium removal from wastewater, *Chem. Eng. J.*, 189–190 (2012) 196–202.
- [33] Y.S. Szeto, Z. Hu, Method for preparing chitosan nano-particles, US 2008/0234477 A1, US 2008/0234477 A1, 2008.
- [34] H. Momenzadeh, A.R. Tehrani-Bagha, A. Khosravi, K. Gharanjig, K. Holmberg, Reactive dye removal from wastewater using a chitosan nanodispersion, *Desalination*, 271 (2011) 225–230.
- [35] H.-C. Yang, W.-H. Wang, K.-S. Huang, M.-H. Hon, Preparation and application of nanochitosan to finishing treatment with anti-microbial and anti-shrinking properties, *Carbohydr. Polym.*, 79 (2010) 176–179.
- [36] L.-M. Zhao, L.-E. Shi, Z.-L. Zhang, J.-M. Chen, D.-D. Shi, J. Yang, Z.-X. Tang, Preparation and application of chitosan nanoparticles and nanofibers, *Brazilian J. Chem. Eng.*, 28 (2011) 353–362.
- [37] C. Yuwei, W. Jianlong, Preparation and characterization of magnetic chitosan nanoparticles and its application for Cu (II) removal, *Chem. Eng. J.*, 168 (2011) 286–292.
- [38] K.S. Huang, W.J. Wu, J.B. Chen, H.S. Lian, Application of low-molecular-weight chitosan in durable press finishing, *Carbohydr. Polym.*, 73 (2008) 254–260.
- [39] APHA, American Public Health Association, Standard Methods for the Examination of Water and Wastewater, Theclassics Us, United States, 2013.
- [40] L. Zhang, A. Manthiram, Chains composed of nanosize metal particles and identifying the factors driving their formation, *Appl. Phys. Lett.*, 70 (1997) 2469–2471.
- [41] M.R. Taha, A.H. Ibrahim, Characterization of nano zero-valent iron (nZVI) and its application in sono-Fenton process to remove COD in palm oil mill effluent, *J. Environ. Chem. Eng.*, 2 (2014) 1–8.
- [42] F. He, D. Zhao, Preparation and characterization of a new class of starch-stabilized bimetallic nanoparticles for degradation of chlorinated hydrocarbons in water, *Environ. Sci. Technol.*, 39 (2005) 3314–3320.
- [43] H. Yuh-Shan, Citation review of Lagergren kinetic rate equation on adsorption reactions, *Scientometrics*, 59 (2004) 171–177.
- [44] S. Lagergren, About the theory of so-called adsorption of soluble substances, *Kungliga Svenska Vetenskapsakademiens Handlingar*, 24 (1898) 1–39.
- [45] A.R. Cestari, E.F.S. Vieira, R.E. Bruns, C. Airoidi, Some new data for metal desorption on inorganic–organic hybrid materials, *J. Colloid. Interf. Sci.*, 227 (2000) 66–70.
- [46] Y.-S. Ho, Comment on equilibrium and kinetics studies of adsorption of copper (II) on chitosan and chitosan/PVA beads, *Int. J. Biol. Macromol.*, 38 (2006) 148–149.
- [47] F.-C. Wu, R.-L. Tseng, R.-S. Juang, Kinetic modeling of liquid-phase adsorption of reactive dyes and metal ions on chitosan, *Water Res.*, 35 (2001) 613–618.
- [48] Y.S. Ho, G. McKay, The kinetics of sorption of divalent metal ions onto sphagnum moss peat, *Water Res.*, 34 (2000) 735–742.
- [49] W.S. Wan Ngah, A. Kamari, Y.J. Koay, Equilibrium and kinetics studies of adsorption of copper (II) on chitosan and chitosan/PVA beads, *Int. J. Biol. Macromol.*, 34 (2004) 155–161.